Available online at www.sciencedirect.com
ScienceDirect
Engineering Structures 29 (2007) 1201–1208
ENGINEERING STRUCTURES
www.elsevier.com/locate/engstruct

Rotational inertia dampers with toggle bracing for vibration control of a building structure

Jae-Seung Hwang[a], Jinkoo Kim[b,*], Young-Moon Kim[c]

[a] School of Architecture, Chonnam National University, Gwangju, Republic of Korea
[b] Department of Architectural Engineering, Sungkyunkwan University, Suwon, Republic of Korea
[c] Department of Architecture and Urban Engineering, Chonbuk National University, Chonju, Republic of Korea

Received 7 February 2006; received in revised form 12 July 2006; accepted 4 August 2006
Available online 2 October 2006

Abstract

This paper presents a new vibration control device by which the equivalent mass and damping of a structure are increased simultaneously. The vibration control system, rotational inertia dampers combined with toggles, can be utilized effectively even in structures with small drift. Numerical analysis shows that the performance of the rotational inertia damper is further enhanced with the addition of a viscous or friction damping mechanism. It is also observed that as the lead of the ball-screw decreases the equivalent mass and damping of the structure and consequently the vibration control effect of the rotational inertia damper increases significantly.

Keywords: Rotational inertia dampers; Toggle bracing; Vibration control; Viscous damping; Friction damping

1. Introduction

Building structures are exposed to various types of vibrations. Especially the wind and the earthquake-induced dynamic effects are considered to be the fundamental problems of structural design. To increase the mass of a structure may be effective in decreasing the wind-induced vibration, in which the external load acts mostly independently of the structure and the increase in the inertia force acts against the wind load. When a structure is subjected to an earthquake ground motion, however, the mass of the structure multiplied by the ground acceleration acts on the structure as an external force. In this case increasing mass of the structure is not desirable. Even for wind load, increasing mass of a structure is not economical. Therefore it would be beneficial if an inertia force is provided in such a way that it is independent of the external load and does not increase the structural mass significantly.

Recently various types of mechanical damping devices have been developed and applied in building structures to mitigate vibration-induced dynamic effects [1–8]. Especially the dampers installed between stories, such as viscous, viscoelastic, friction, and hysteretic dampers, are mostly intended to dissipate vibrational energy by enhancing the damping of structures. As building structures are much larger and heavier than the machines or electronic devices that need vibration control, the size and the required control force of dampers are usually much larger than those of devices applied in machines. Also as the responses of structures are relatively small and as the control force of dampers is in many cases generated proportionally to the responses, the size of the dampers needs to be large enough to generate the required control force. However as the size of a damper increases the cost of manufacturing, transportation, installation, and maintenance also increases. Therefore the size of a damper is required to be kept as small as possible.

The toggle bracing system works to magnify the deformation and control efficiency of a damper. It has been used in various mechanical devices such as stone crushers, punch presses, impact reducers, etc. [9]. In civil or building structure fields, researchers including Hibino et al. [10], Constantinou et al. [11,12], Kang [13], and Gluck et al. [14] have developed various types of toggle bracing configurations. In previous research the

* Corresponding address: Department of Architectural Engineering, Chunchun-Dong, Jangan-Gu, Suwon, Kyunggi-Do, Republic of Korea. Tel.: +82 31 290 7563; fax: +82 31 290 7570.
E-mail address: jkim@skku.edu (J. Kim).

0141-0296/$ - see front matter © 2006 Elsevier Ltd. All rights reserved.
doi:10.1016/j.engstruct.2006.08.005

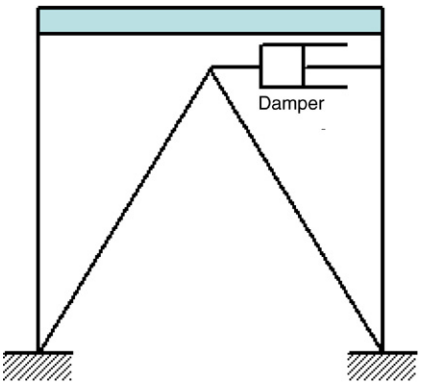

(a) Chevron brace.

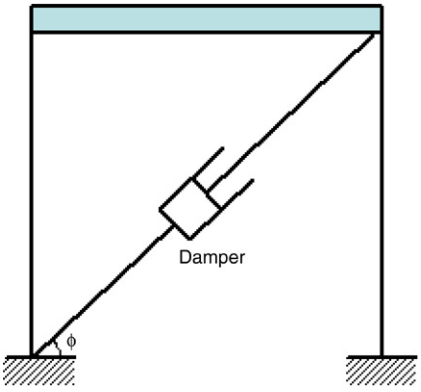

(b) Diagonal brace.

Fig. 1. Configuration of a damper with supporting brace.

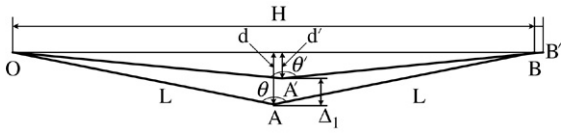

Fig. 2. Magnification of displacement by toggle bracing.

steel braces were usually considered as a rigid body in the process of structural analysis. However most mechanical dampers have stiffness to some degree and the amplification of displacement by toggle bracing may depend on the relative stiffness of the damper and the toggle brace. This needs to be further investigated to compute the magnification effect more accurately.

In this study the validity of a new mechanical damper, the rotational inertia damper, is investigated through numerical analysis. Once installed between stories, the damper provides effective mass to the structure expressed as the rotational mass moment of inertia multiplied by the inverse of the ball screw lead squared. Viscous and friction damping mechanisms are also added to increase the effective damping of the structure. The efficiency of the damper is further enhanced by connecting the damper to a toggle bracing to magnify the relative displacement. The effect of the relative stiffness between the damper and the toggle on the magnification of displacement is also investigated.

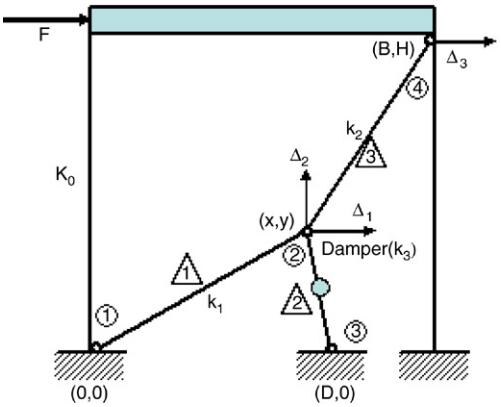

Fig. 3. Damper–toggle bracing configuration.

2. Toggle brace systems

2.1. Amplification ratio of a single-toggle system

In building structures, the chevron-type or diagonal braces are generally adopted for installing dampers between stories (Fig. 1). In the case the inter-story drift is Δ, the relative displacements of the chevron brace, Δ_c, and the diagonal brace, Δ_d, are as follows:

$$\Delta_c = \Delta \tag{1a}$$

$$\Delta_d = \cos(\phi)\Delta \tag{1b}$$

where ϕ is the slope of the brace. In Fig. 2 the horizontal displacement of the structure, Δ, induces the vertical displacement of the toggle system, Δ_1; the amplification ratio, $\frac{\Delta_1}{\Delta}$, depends on the length of the two links and the angle θ between them. When the lengths of the two links are the same, the relation between Δ and Δ_1 are obtained from the following equation:

$$\left(\frac{\Delta}{2L} + \sin\left(\frac{\theta}{2}\right)\right)^2 + \left(\frac{\Delta_1}{L} - \cos\left(\frac{\theta}{2}\right)\right)^2 = 1. \tag{2}$$

In the case the lateral displacement is much smaller than the length of the links, Eq. (2) can be reduced to

$$A = \frac{\Delta_1}{\Delta} = \frac{1}{2}\tan\left(\frac{\theta}{2}\right). \tag{3}$$

There are various configurations of toggle bracing developed [11]; the previous research on toggle bracing generally assumed the links as rigid bodies. This assumption may hold when the stiffness of the connected dampers is small enough to be neglected. However only the dampers with no stiffness, such as viscous dampers, will meet the assumption. For devices with stiffness, such as viscoelastic or friction dampers, the amplifying effect of toggle systems can be overestimated if the stiffness of a damper is not considered. The effect of damper stiffness on the amplification ratio of a toggle system is investigated with the simple toggle bracing shown in Fig. 3. The story stiffness

Table 1
Properties of the SDOF structure with a toggle brace

Properties	Symbols	Values
Width	B	4 m
Height	H	4 m
Location of toggle	(x, y)	(1.74, 2.26) m
Location of damper	$(D, 0)$	(3, 0) m
Cross-section of toggle brace	A	63.5E–4
Elastic modulus	E	210 GPa
Length of brace	L	2.85 m
Stiffness of brace	k_1, k_2 (EA/L)	4.68E8 N/m
Story stiffness	K_0	1.28E6 N/m
Magnification ratio (stiffness ratio = 0)	Amp	2.79

of the structure is K_0; all connections are considered as hinges; and the links are modeled as truss elements. When the stiffness of the damper is negligible ($k_3 = 0$), the lateral displacement Δ_3 is obtained as follows:

$$\Delta_3 = \frac{F}{K_0}. \tag{4}$$

When the stiffness of the damper is considered, the displacements are obtained as follows

$$\begin{pmatrix} k_1c_1^2 + k_2c_2^2 + k_3c_3^2 & k_1c_1s_1 + k_2c_2s_2 + k_3c_3s_3 & -k_2c_2^2 \\ k_1c_1s_1 + k_2c_2s_2 + k_3c_3s_3 & k_1s_1^2 + k_2s_2^2 + k_3s_3^2 & -k_2s_2c_2 \\ -k_2c_2^2 & -k_2s_2c_2 & k_2c_2^2 + K_0 \end{pmatrix} \times \begin{bmatrix} \Delta_1 \\ \Delta_2 \\ \Delta_3 \end{bmatrix} = \begin{bmatrix} 0 \\ 0 \\ F \end{bmatrix} \tag{5}$$

where c_i, s_i, are the sine and cosine values of the angle between the ith member and the floor:

$$c_1 = \frac{x}{\sqrt{x^2 + y^2}} \tag{6a}$$

$$s_1 = \frac{y}{\sqrt{x^2 + y^2}}. \tag{6b}$$

The amplification ratio of the toggle brace, i.e. the deformation of the damper divided by the displacement of the structure, can be expressed as follows

$$A = \frac{\sqrt{(x + \Delta_1 - D)^2 + (y + \Delta_2)^2} - \sqrt{(x - D)^2 + y^2}}{\Delta_3}. \tag{7}$$

Fig. 4 plots the amplification ratio of the system for various stiffness ratios of the damper and the toggle brace defined as k_3/k_1 or k_3/k_2. The properties of the system to be used in the analysis are shown in Table 1. It is assumed that the stiffness of toggle braces is the same, that is, $k_1 = k_2$. When the stiffness of the damper is zero, the amplification ratio is 2.79. It can be observed that as the stiffness of the damper increases the amplification ratio decreases, and when the damper stiffness is equal to that of the toggle bracing, the amplification ratio becomes less than one, which implies that the toggle has negative effect on the amplification of displacement. The conventional procedure of neglecting damper stiffness is valid only when the stiffness of the toggle brace is 10 000 times

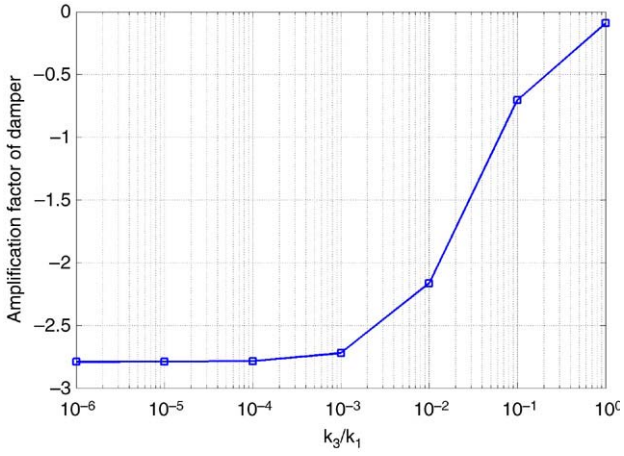

Fig. 4. Amplification of displacement for various stiffness ratios of the damper and the toggle brace.

greater than that of the damper. Therefore it would be necessary to design a toggle bracing system considering the effective stiffness of dampers connected.

2.2. Double-toggle bracing system

In the conventional toggle system composed of a toggle bracing and a damper (Fig. 3), the angle between the two links is generally maintained close to 180° to maximize the amplification effect of relative displacement. In this case, however, the maximum deformation capacity of the toggle system can be exceeded when an external force larger than the design force acts on the structure. For example, the maximum deformation capacity of a toggle–damper system optimally designed for wind load with 10-year return period may be exceeded when a wind load of 100-year return period or large earthquake load are applied on the structure. In this case the toggle–damper system behaves more like a diagonal brace rather than a damping device. This shortcoming can be overcome by using a multiple toggle bracing configuration, in which the same or different types of multiple dampers are installed with multiple toggle braces as shown in Fig. 5. It has the advantage of operating even after the maximum deformation capacity is reached. As the multiple toggle bracing is composed of shorter links, the system has higher buckling strength than the conventional single-toggle bracing. This

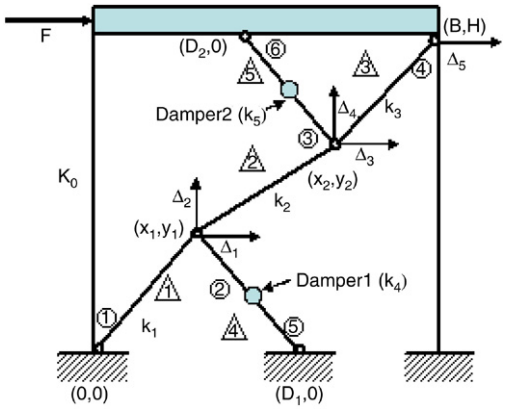

Fig. 5. Double-toggle bracing configuration.

Table 2
Properties of the SDOF structure with a double-toggle brace

Properties	Symbols	Values
Location of toggle for damper 1	$(x1, y1)$	(1.22, 1.46) m
Location of damper 1	$(D1, 0)$	(2, 0) m
Location of toggle for damper 2	$(x2, y2)$	(2.78, 2.54) m
Location of damper 2	$(D2, 0)$	(2, 4) m
Length of brace	L	1.9 m
Stiffness of brace	k_1, k_2, k_3 (EA/L)	7.02E8 N/m
Story stiffness	K_0	1.28E6 N/m
Stiffness of dampers	$k4, k5$	–

also leads to higher link-damper stiffness ratio, resulting in higher amplification of displacement. Another advantage is that smaller dampers can be used to generate the same damping force as that of a single-toggle system. In Fig. 5 the amplified displacements of the two dampers can be computed from the following force–displacement relationship:

$$K\Delta = F \tag{8}$$

where K is the 5×5 stiffness matrix, and Δ and F are the 5×1 vectors of the displacements and the external force, respectively:

$$\Delta = [\Delta_1 \quad \Delta_2 \quad \Delta_3 \quad \Delta_4 \quad \Delta_5]^{\mathrm{T}} \tag{9a}$$

$$F = [0 \quad 0 \quad 0 \quad 0 \quad F_5]^{\mathrm{T}}. \tag{9b}$$

After solving Eq. (8), the displacement amplification ratios for the two dampers are obtained as follows:

$$A_1 = \frac{\sqrt{(x_1 + \Delta_1 - D_1)^2 + (y_1 + \Delta_2)^2} - \sqrt{(x_1 - D_1)^2 + y_1^2}}{\Delta_5} \tag{10a}$$

$$A_2 = \frac{\sqrt{(x_2 + \Delta_3 - D_2 - \Delta_5)^2 + (y_2 + \Delta_4 - H)^2} - \sqrt{(x_2 - D_2)^2 + (y_2 - H)^2}}{\Delta_5} \tag{10b}$$

where Δ_5 is the relative displacement of the structure. Table 2 shows the properties of the toggle bracing used to compute the amplification ratios for varying stiffness of dampers. The values already given in Table 1 are not shown in Table 2. Fig. 6 shows the amplification ratio for each damper for various damper stiffness ratios (k_5/k_4) when the stiffness ratio of the

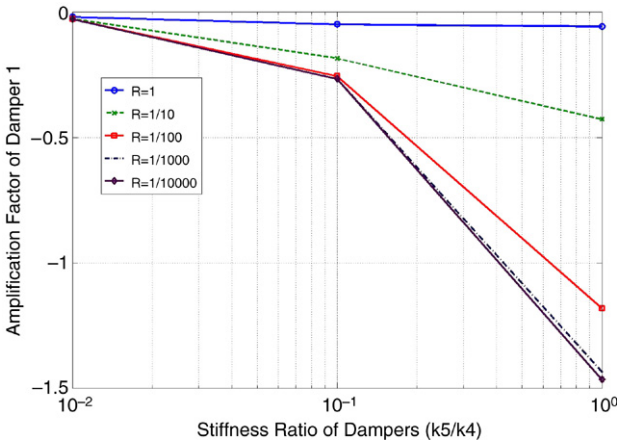

(a) Amplification ratio for damper 1.

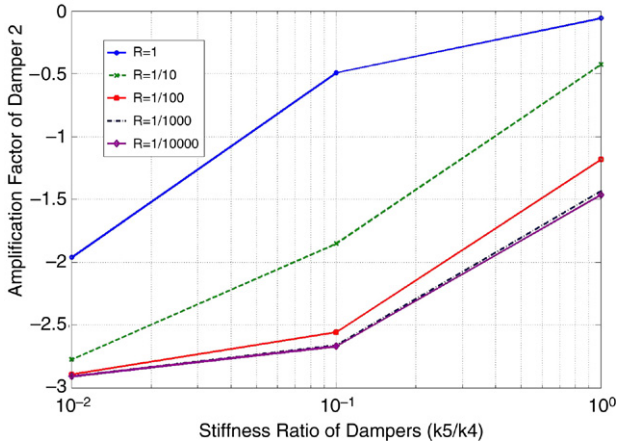

(b) Amplification ratio for damper 2.

Fig. 6. Amplification of relative displacement of the dampers for various stiffness ratios of dampers.

links and the damper 1, R, is fixed to 1.0, 1/10, 1/100, 1/1000, and 1/10 000. The negative amplification ratio implies that the dampers are under compression. It can be observed that as R decreases the amplification ratio increases and that the amplification ratio converges to a certain value as R decreases less than 1/1000. Also as the damper stiffness ratio decreases the displacement amplification of damper 1 decreases while that of damper 2 increases. This implies that when the stiffness of the two dampers are quite different, the stiffer one behaves like a rigid body and the displacement of the less stiff one is greatly amplified. When the stiffness of the dampers are identical, the amplification ratios also become identical.

3. Rotational inertia dampers

In the rotational inertia damper (RID) shown schematically in Fig. 7, the inter-story drift of a structure is transformed to rotational movement in the damper by a ball screw, and kinetic energy is generated in the system by a rotating mass in the damper. Input energy can be dissipated either by viscous fluid, such as silicon oil, filled in the damper (rotational inertia–viscous dampers, RIVD) or by friction between the rotating mass and the external tube (rotational

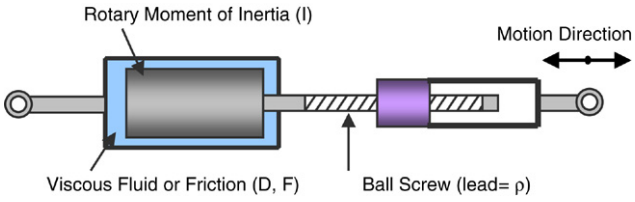

Fig. 7. Configuration of a rotational inertia viscous damper.

inertia–friction dampers, RIFD). In this study the equations of motion governing the dynamic behavior of the rotational dampers are derived, and their vibration reduction capacities are investigated. Also the enhancement of the vibration control effect is observed when the dampers are used combined with a toggle bracing system.

3.1. Rotational inertia–viscous dampers

In the derivation of the equation of motion of a single-degree-of-freedom (SDOF) system with a RIVD, it is assumed that the damping force is proportional to the speed of the rotating mass. Then the kinetic energy (T), potential energy (V), and the variation of the dissipated energy due to the damper (δW) are expressed as follows:

$$T = \frac{1}{2}M\dot{x}^2 + \frac{1}{2}I\dot{\omega}^2 \tag{11a}$$

$$V = \frac{1}{2}Kx^2 \tag{11b}$$

$$\delta W = -F_d\delta\omega = -D\dot{\omega}\delta\omega \tag{11c}$$

where M and K are the mass and the stiffness of the SDOF system; x is the displacement of the system; ω and I are the rotation and the rotational moment of inertia of the mass in the damper, respectively; and δ represents the variation. D is the damping coefficient determined by various factors such as the lead of the ball screw, size of the rotating mass, viscosity of the viscous fluid, distance between the rotating mass and the external tube. The displacement x and the rotation ω are related as follows:

$$\omega = \frac{2\pi}{\rho}x \tag{12}$$

where ρ is the lead of the ball screw. The equation of motion of the SDOF system with RIVD is obtained as follows using the Lagrange method [15]:

$$M\ddot{x} + C\dot{x} + Kx = -I\frac{4\pi^2}{\rho^2}\ddot{x} - D\frac{4\pi^2}{\rho^2}\dot{x} + F(t) \tag{13}$$

where C is the inherent damping coefficient $F(t)$ and is the external load not included in Eq. (11) for simplicity. From the right-hand-side of the above equation, the control force of the damper, U_d, is separated as follows:

$$U_d = -I\frac{4\pi^2}{\rho^2}\ddot{x} - D\frac{4\pi^2}{\rho^2}\dot{x} \tag{14}$$

where it can be observed that the control force is contributed from the rotational moment of inertia as well as the damping coefficient of the damper. This is the special form of the slope-state feedback control. The equation of motion of Eq. (13) is rewritten as follows

$$\left(M + I\frac{4\pi^2}{\rho^2}\right)\ddot{x} + \left(C + D\frac{4\pi^2}{\rho^2}\right)\dot{x} + Kx = F(t). \tag{15}$$

Dividing each side of Eq. (15) by the mass of the structure, M, leads to:

$$\left(1 + \frac{I}{M}\frac{4\pi^2}{\rho^2}\right)\ddot{x} + \left(2\xi_0\omega_0 + \frac{D}{M}\frac{4\pi^2}{\rho^2}\right)\dot{x} + \omega_0^2 x = \bar{f}(t) \tag{16}$$

where $\bar{f}(t) = F(t)/M$ corresponds to ground acceleration in the case of earthquake load. In this case x is the relative displacement of the structure. Eq. (16) is further simplified as follows

$$(1+\mu)\ddot{x} + 2(\xi_0 + \xi_d)\omega_0\dot{x} + \omega_0^2 x = \bar{f}(t) \tag{17a}$$

where the equivalent mass ratio μ and the equivalent damping ratio ξ_d are expressed as

$$\mu = \left(\frac{I}{M}\frac{4\pi^2}{\rho^2}\right), \qquad \xi_d = \left(\frac{D}{M}\frac{2\pi^2}{\rho^2}\frac{1}{\omega_0}\right). \tag{17b}$$

It can be observed that the equivalent mass and damping increase inversely proportional to the ball screw lead squared.

3.2. Control force of the rotational inertia–viscous damper with toggle bracing

When a RIVD is installed with a toggle bracing in a story, the relationship between the relative displacement of the damper is expressed as a function of the story drift, x, as follows:

$$d = f(x) \tag{18a}$$

where the function f has the form of Eq. (10), for example. The relative velocity and acceleration at the ends of the damper are obtained as

$$\upsilon = \frac{\mathrm{d}f}{\mathrm{d}x}\frac{\mathrm{d}x}{\mathrm{d}t} = \frac{\mathrm{d}f}{\mathrm{d}x}\dot{x} \tag{19a}$$

$$a = \frac{\mathrm{d}}{\mathrm{d}t}(\upsilon) = \left(\frac{\mathrm{d}^2 f}{\mathrm{d}x^2}\right)\dot{x}^2 + \frac{\mathrm{d}f}{\mathrm{d}x}\ddot{x}. \tag{19b}$$

The control force of a rotational inertia–viscous damper with toggle bracing can be expressed as follows using the Lagrange equation of Eq. (11) and the variation of the relative displacement of the structure, δx:

$$U_d = -I\frac{4\pi^2}{\rho^2}\left[\left(\frac{\mathrm{d}^2 f}{\mathrm{d}x^2}\dot{x}^2\right) + \frac{\mathrm{d}f}{\mathrm{d}x}\ddot{x}\right]\left(\frac{\mathrm{d}f}{\mathrm{d}x}\right) - D\frac{4\pi^2}{\rho^2}\left[\frac{\mathrm{d}f}{\mathrm{d}x}\dot{x}\right]\left(\frac{\mathrm{d}f}{\mathrm{d}x}\right). \tag{20}$$

Compared with Eq. (14), which presents the control force of a RIVD, it can be observed that the control force is increased as a result of the installation of toggle bracing.

Table 3
Dynamic characteristics of the SDOF structure and the damper

		Symbol	Value
Structure	Mass	M	14.58 ton
	Stiffness	K	1.28 E6 N/m
	Damping constant	C	3.11 E3 N s/m
	Natural	f_0	1.49 Hz
	frequency	ω_0	9.3697 rad
	Damping ratio	ξ_0	1.14%
	Height	H	4 m
RIVD	Rotational moment of inertia	I	0.02 kg m^2
	Viscous damping constant	D	0.083 N m s
RIFD	Friction damping constant	To	8.32 N m
Ball screw	Lead	ρ	2 cm, 4 cm

3.3. Control force of a rotational inertia–friction damper with toggle bracing

The RIFD with toggle bracing dissipate vibration energy by friction between the rotational mass and the external tube of the damper. When such a damper is installed in a SDOF system, the variation of the dissipated energy is obtained as follows:

$$\delta W = -F_d \delta\omega = -\frac{2\pi}{\rho} T_0 \,\mathrm{sign}(\dot{x})\delta x \tag{21}$$

where sign(.) is the sign function and T_0 is the friction force that is generated when the mass in the damper rotates one full turn. When the relative velocity and the acceleration acting on the damper are given as Eq. (19), the control force of a RIFD with toggle bracing is obtained as follows:

$$U_d = -I\frac{4\pi^2}{\rho^2}\left[\left(\frac{\mathrm{d}^2 f}{\mathrm{d}x^2}\dot{x}^2\right) + \frac{\mathrm{d}f}{\mathrm{d}x}\ddot{x}\right]\frac{\mathrm{d}f}{\mathrm{d}x} - \frac{2\pi}{\rho} T \,\mathrm{sign}(\dot{x})\left[\frac{\mathrm{d}f}{\mathrm{d}x}\right]. \tag{22}$$

In comparison with Eq. (20), which shows the control force of a RIVD with toggle bracing, the control forces of RIVD and RIFD contributed from rotational inertia are the same. However the control forces caused by the viscous and the friction damping are different.

4. Numerical examples

Numerical analysis has been carried out to verify the vibration control effect of the damper after substituting Eq. (20) or Eq. (21) into the control force in Eq. (13). Table 3 presents the properties of the structure and the damper–toggle system used in the analysis. Four types of structures are considered: (1) structure without any damper; (2) structure with RID–toggle bracing; (3) structure with RIVD–toggle bracing; and (4) structure with RIFD–toggle bracing. The control force of a pure rotational inertia damper without viscous or friction damping can be obtained by neglecting the viscous damping term in Eq. (20). The time history of the El-Centro (NS) earthquake is used as an input load.

Fig. 8(a) compares the time history of the displacement response of the structure with and without the damper. The lead

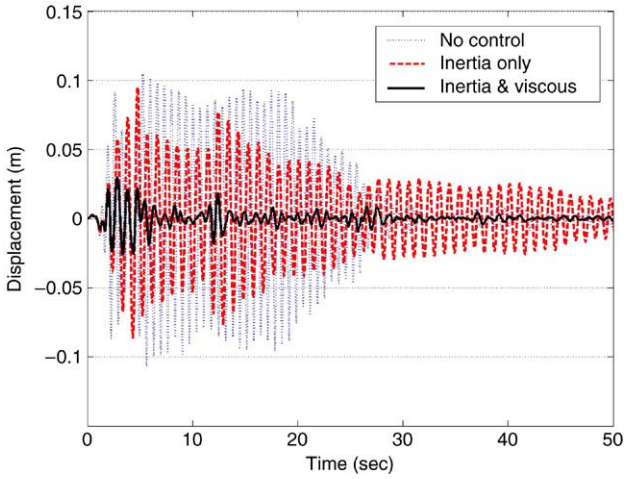

(a) Displacement.

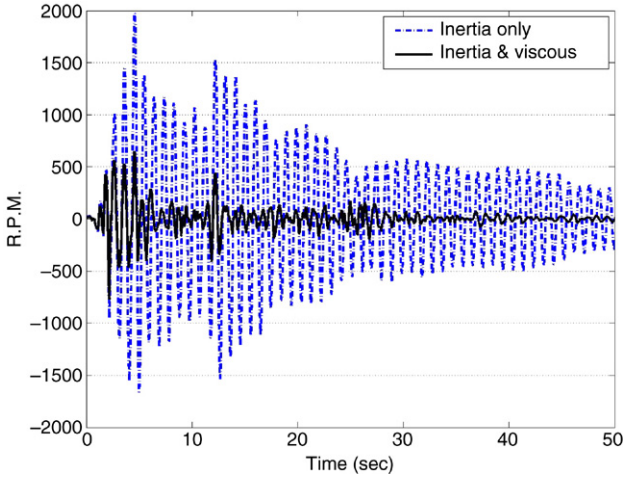

(b) Speed of the rotating mass in the damper.

Fig. 8. Response time histories of the model structure (lead = 2 cm).

of the ball screw is set to be 2 cm. It can be observed that, compared with the response of the structure without damper, the response of the structure decreases with the installation of the RID. The response further decreases when a viscous damping mechanism is introduced to the rotational inertia damper. Fig. 8(b) compares the speed of the rotating mass in the damper with and without viscous fluid in the form of revolutions per minute (RPM), where it can be observed that the mass rotates much faster when there is no viscous damping involved.

Fig. 9(a) shows the displacement time history of the structure with RIVD and RIFD. In numerical simulation it would be meaningless to compare the controllability of the two dampers with different energy-dissipation mechanisms, because it is possible to adjust the coefficients of viscous and friction damping to the same controllability. However the difference in vibration control mechanism between the two dampers can be observed in the figure; the friction damping mechanism starts to activate only when the displacement exceeds a certain threshold value. Fig. 9(b) compares the speed of the rotating mass in the dampers, in which it can be seen that the mass in the RIFD rotates faster in the beginning, but soon becomes slower than

Table 4
Equivalent mass and damping contributed from the rotational inertia dampers

Lead of ball screw		RIVD		RIFD	
		2 cm	4 cm	2 cm	4 cm
Mass	Structure mass	14.58 ton		14.58 ton	
	Rotational inertia	0.02 kg m^2		0.02 kg m^2	
	Equiv. mass without toggle	1.97 ton	0.49 ton	1.97 ton	0.49 ton
	Equiv. mass with toggle	15.35 ton	3.84 ton	15.35 ton	3.84 ton
	Equiv. mass/structure mass	105%	26%	105%	26%
	Natural frequency	1.04 Hz	1.33 Hz	1.04 Hz	1.33 Hz
Damping	Inherent damping	3.11 kN s/m		3.11 kN s/m	
	Damping constant	0.083 N m s		8.32 N m	
	Damping coefficient without toggle	8.18 kN s/m	2.05 kN s/m	2.61 kN	1.31 kN
	Damping coefficient with toggle	63.69 kN s/m	15.92 kN s/m	7.29 kN	3.65 kN
	Equivalent damping ratio	17.1%	6.2%	–	–

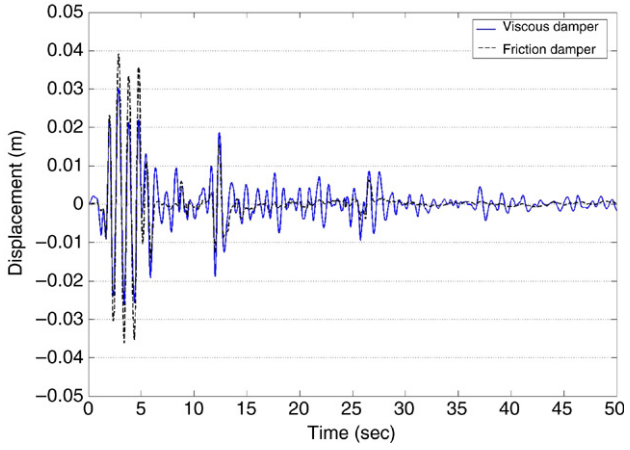

(a) Displacement.

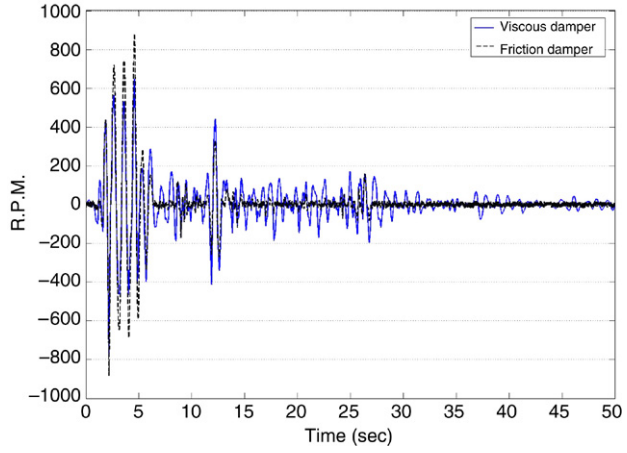

(b) Speed of the rotating mass in the damper.

Fig. 9. Response time history of the structure with RIVD and RIFD.

that of the RIVD. This is consistent with the observation of Fig. 9(a); in the first stage of vibration, the larger displacement of the structure with RIFD results in higher speed of the rotating mass in the RIFD. Once the friction damping mechanism is activated and the displacement becomes smaller, the speed of the rotating mass also becomes smaller than that of the mass in the RIVD.

Table 5
Reduction of maximum responses due to installation of a damper with toggle bracing

	Max. displacement (cm) (reduction ratio)		Max. velocity (cm/s) (reduction ratio)		RPM	
	$\rho = 2$	$\rho = 4$	$\rho = 2$	$\rho = 4$	$\rho = 2$	$\rho = 4$
No damper	10.7		97.3			
RID	9.5 (11%)	8.0 (25%)	65.9 (32%)	60.9 (37%)	1976	913
RIVD	3.0 (72%)	6.1 (41%)	25.7 (74%)	52.6 (46%)	771	788
RIFD	3.9 (62%)	7.1 (34%)	29.4 (70%)	57.3 (41%)	881	858

The equivalent mass and damping contributed from the rotational dampers are computed from Eqs. (20) and (22) and are shown in Table 4. The equivalent mass depends on the rotational mass and does not change with the introduction of the energy dissipation mechanism. It can be seen that as the lead of the ball screw decreases the equivalent damping and mass increase. If the relative displacement of the structure is amplified by the toggle brace, the equivalent mass and damping are also amplified significantly. When the lead is 2 cm, the equivalent mass contributed from the rotating mass corresponds to as high as 105% of the structure mass. It can be noticed that the natural frequency decreases from 1.49 Hz to 1.04 Hz when the lead is 2 cm, mainly contributed from the addition of the equivalent mass. As the viscous damper is a linear system, the equivalent damping ratio can be obtained from Eq. (16). When the lead is 2 cm and the damping constant of the RIVD is 0.083 N m s, the equivalent damping ratio of the structure increases from 1.14% to 17% after installation of the RIVD–toggle bracing system.

Table 5 presents the maximum responses of the model structure with and without the dampers. In all cases the damper is used in combination with the toggle bracing. It can be seen that the maximum displacement and velocity reduce by 11%

and 32%, respectively, when the rotational inertia dampers with ball screw lead of 2 cm are applied; and by 25% and 37% when the damper with the lead length of 4 cm are used. If viscous or friction mechanism is applied in addition to the rotational inertia, the vibration reduction effect becomes more significant; for example, the reduction ratio increases from 11% to 72% when viscous damping is included in the rotational inertia damper. As can be observed in Eqs. (20) and (22) and as confirmed in Table 4, the equivalent mass and damping increase as the length of the ball screw lead decreases. However, contrary to the above observation, the reduction ratios for the displacement and velocity are higher when the length of the lead is 4 cm than when the length of the lead is 2 cm in the case the RID is employed. This can be considered as the characteristic of the inertia damper without any damping mechanism, and can be explained as follows: the increase in the equivalent mass results in a decrease in the natural frequency; if the natural frequency happens to move closer to the dominant frequency of the external load, the responses can be magnified even though the length of the lead decreases. When an energy dissipation mechanism is introduced, however, this phenomenon does no longer visible because the effect of energy dissipation is dominant over the contribution from the changed natural frequency. Finally it can be observed in the table that when the RID is used without an energy dissipation mechanism, the speed of the rotating mass increases more than twice when the lead of the ball screw decreases to 2 cm. However when viscous or frictional force is involved, it is observed that the speed of the rotating mass no longer depends on the length of the lead. This can be explained as follows: with a shorter lead of the ball screw the rotating speed of the mass increases; this enhances the energy dissipation mechanism and consequently the displacement of the structure and the speed of the rotating mass decrease.

5. Conclusions

This study investigated the vibration control effect of a rotational inertia damper combined with a toggle bracing through numerical analysis. The results are summarized as follows:

(1) The efficiency of a toggle bracing depends heavily on the relative stiffness of the damper and the brace, and the displacement-magnification effect is maximized when the stiffness ratio of the damper/brace is less than 1/10 000. The effectiveness of a double-toggle bracing system varied with stiffness ratio of the two dampers.

(2) The rotational inertia damper combined with various energy-dissipating mechanisms turned out to be effective in reducing structural vibration. The efficiency of the damper depended heavily on the length of the ball screw lead; as the lead decreased, the effective mass, effective damping, and consequently the effectiveness of the damper increased significantly.

Acknowledgements

This work was supported by the NRL (National Research Laboratory) Program of the Ministry of Science and Technology and the Regional Research Centers Program (Biohousing Research Institute) granted by the Korean Ministry of Education & Human Resources Development.

References

[1] Meirovitch L. Dynamics and control of structures. NY: John Wiley & Sons; 1990.
[2] Dyke SH, Spencer Jr BF, Quast P, Sain MK, Kaspari Jr DC, Soong TT. Experimental verification of acceleration feedback control strategies for the active tendon system. Technical report NCEER-94-0024. Buffalo (NY): State University of New York; 1994.
[3] Tsuji M, Nakamura T. Optimum viscous dampers for stiffness design of shear buildings. Structural Design of Tall Buildings 1996;5:217–34.
[4] Chang KC, Soong TT, Oh ST, Lai ML. Seismic behavior of steel frame with added viscoelastic dampers. Journal of Structural Engineering 1995; 121(10):1418–26.
[5] Spencer BF, Dyke SJ, Deoskar HS. Benchmark problems in Structural control: Part I—active mass driver system. Earthquake Engineering and Structural Dynamics 1998;27:1125–39.
[6] McNamara RJ. Tuned mass dampers for buildings. Journal of the Structural Division ASCE 1977;103:ST9.
[7] Lee SH, Min KW, Hwang JS, Kim J. Evaluation of equivalent damping ratio of a structure with added dampers. Engineering Structures 2004;26: 335–46.
[8] Hwang JS, Lee SH, Min KW, Kim J. Equivalent damping of a structure with vibration control devices subjected to wind loads. Wind and Structures 2003;6:249–62.
[9] Sclater N, Chirois NP. Mechanisms and mechanical devices source book. 3rd ed. McGraw-Hill; 2001. p. 211–2.
[10] Hibino H, Kawamura S, Hisano M, Yamada M, Kawamura H, Morita H. A study on response control system on structures utilizing damping amplifier. Taisei Technical Research Journal 1989;22:155–62.
[11] Constantinou MC, Tsopelas P, Hammel W, Sigaher AN. Toggle-brace-damper seismic energy dissipation system. Journal of Structural Engineering, ASCE 2001;127(2):105–12.
[12] Constaninou MC, Sigaer AN. Energy dissipation system configurations for improved performance, In: Proceedings of the 2000 structures congress and exposition, ASCE. 2000.
[13] Kang SD, Hong SM, Hwang JS, Joo SJ, Park JH, Lee SH. Vibration control of structures using semi-active control device. Proceedings of Architectural Institute of Korea 1997;17:413–6.
[14] Gluck J, Ribakov Y. Active viscous damping system with amplifying braces for control of MDOF structures. Earthquake Engineering and Structural Dynamics 2002;31:1735–51.
[15] Meirovitch L. Methods of analytical dynamics. McGraw-Hill; 1970. p. 72–88.